

Supplementary Information

Facilely Fabricated Luminescent Nanoparticle Thermosensor for Real-Time Microthermography in Living Animals

Ferdinandus,^{†,||} Satoshi Arai,^{‡,§,||} Shinji Takeoka,^{‡,§,⊥}
Shin'ichi Ishiwata,[#] Madoka Suzuki,^{*,‡,§,¶} and Hirotaka Sato^{*,†}

[†] School of Mechanical and Aerospace Engineering, Nanyang Technological University, Singapore 639798, Singapore

[‡] Waseda Bioscience Research Institute in Singapore (WABIOS), Singapore 138667, Singapore

[§] Comprehensive Research Organization, Waseda University, Shinjuku, Tokyo 162-0041, Japan

[⊥] Department of Life Science and Medical Bioscience, Faculty of Science and Engineering, Waseda University, Shinjuku, Tokyo 162-8480, Japan

[#] Department of Physics, Faculty of Science and Engineering, Waseda University, Shinjuku, Tokyo 169-8555, Japan

[¶] PRESTO, Japan Science and Technology Agency, Kawaguchi, Saitama 332-0012, Japan

^{||} These authors contributed equally to this work

^{*} Corresponding Authors: M. Suzuki. E-mail: suzu_mado@aoni.waseda.jp; H. Sato. E-mail: hirosato@ntu.edu.sg

Table of Contents:

Table S1. Temperature rise of flight muscle during the preflight preparation after RNT loading.....	S3
Figure S1. Illustration of stereo-microscopy, laser and infrared camera setups.....	S4
Figure S2. EuDT luminescence intensity decreased in aqueous condition	S4
Figure S3. UV-vis absorption spectra of the RNT of EuDT and rhodamine 800 embedded PS-MA particles and PS-MA particles without dyes.....	S5
Figure S4. The <i>in vitro</i> normalized luminescence ratio (I_{615}/I_{710}) plotted against the varied temperatures (21.5 to 32.0 °C).....	S5
Figure S5. The <i>in vitro</i> normalized luminescence ratio (I_{615}/I_{710}) plotted against the varied temperatures (21.5 to 44.0 °C).....	S6
Figure S6. The reversibility of the RNT response against the heating-cooling cycle	S6
Figure S7. Reversibility of the luminescence ratio (I_{615}/I_{710}) of the RNT under N ₂ saturated solution.....	S7
Figure S8. Stability of the RNT at higher temperatures for 60 minutes observation.....	S7
Figure S9. Stability of the RNT in MOPS buffer with different pH.....	S8
Figure S10. The averaged <i>in vivo</i> normalized luminescence ratio (I_{615}/I_{710}) plotted against the varying temperature from flight muscles of different beetles during the heating and cooling.....	S9
Figure S11. Infrared thermogram of beetle flight muscle during the preflight preparation, 2 days after RNT loading.....	S9
Figure S12. The spreading of the normalized ΔR values under similar temperature change (ΔT) in the <i>in vivo</i> experiments.....	S10

Table S1. Temperature rise of flight muscle during the preflight preparation after RNT loading.

Elapsed time after RNT loading / day	ΔT (°C)			
	Control	1x concentrated RNT	10x concentrated RNT	100x concentrated RNT
1	2.47 ± 1.12	2.77 ± 0.65	3.80 ± 0.54	3.57 ± 0.94
2	3.88 ± 1.74	4.83 ± 1.55	4.30 ± 1.53	6.10 ± 1.20

The treated beetles were loaded with 20 μL of different concentrations of RNT while the control beetles were loaded with 20 μL of H_2O . The temperature was monitored using an infrared camera. The beetles still displayed temperature rise, even after 2 days of loading of the RNT. There is no detectable lethality due to the RNT loading ($N = 12$ beetles, 3 beetles for each condition).

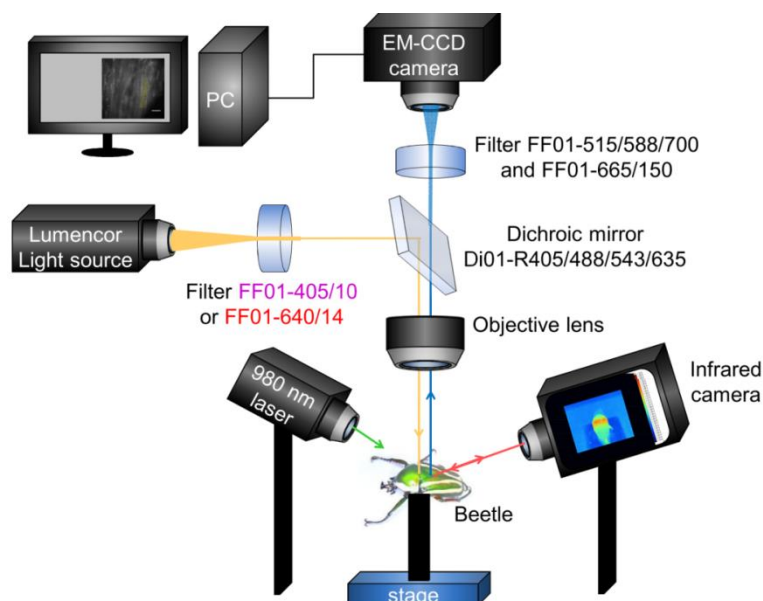


Figure S1. Illustration of stereo-microscopy, laser and infrared camera setups. The excitation filter in purple font was used to excite EuDT whereas the excitation filter in red font was used to excite rhodamine 800. The beetle was tethered on top of a stick which was fixed to a metallic stage. The flight muscle was exposed and observed under stereo microscopy. External heating was induced by using a 980 nm laser. The temperature of the muscle was monitored by an infrared camera.

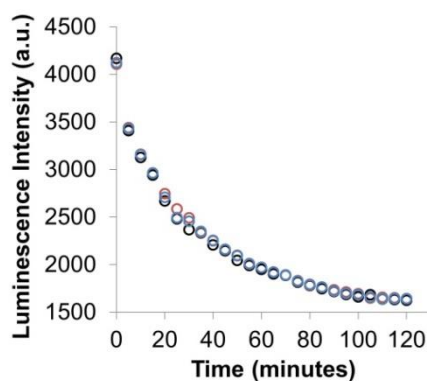


Figure S2. EuDT luminescence intensity decreased in aqueous condition (5% DMSO in Milli-Q water). Luminescence intensity of EuDT (I_{615}) is plotted against the measurement time ($n = 3$ trials, different colours represent independent trials).

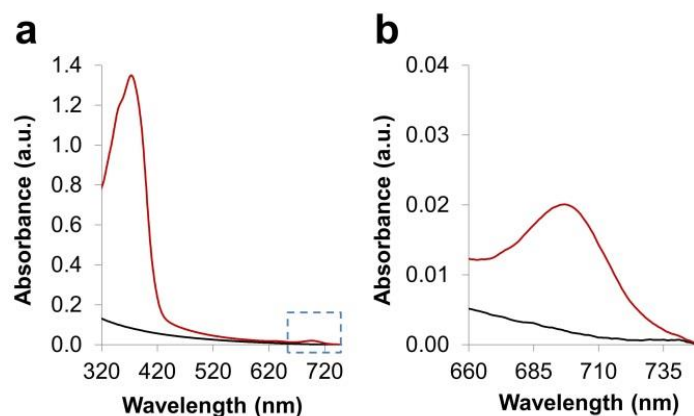


Figure S3. UV-vis absorption spectra of the RNT of EuDT and rhodamine 800 embedded PS-MA particles (red lines) and PS-MA particles without dyes (black lines). Graph plotted were the average of multiple measurements ($n = 5$ measurements). (a) The peak at 370 nm shows the EuDT absorption. The blue rectangular indicates the rhodamine 800 absorption as displayed in the magnified image in (b). (b) The peak at 700 nm shows the absorption of rhodamine 800 in the prepared RNT.

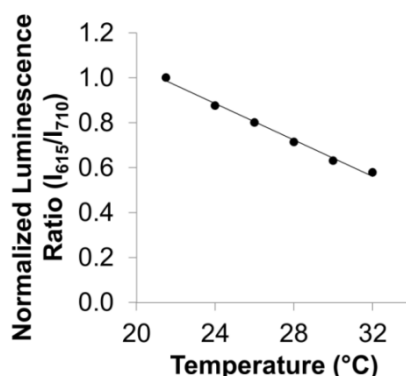


Figure S4. The *in vitro* normalized luminescence ratio (I_{615}/I_{710}) plotted against the varying temperature, with the absolute luminescence ratio shown in Fig. 1e. The ratio at each temperature was normalized by the ratio at 21.5 °C. The temperature sensitivity, or the gradient of the normalized ratio curve is $-4.0\%/^{\circ}\text{C}$ relative to 21.5 °C ($y = -0.040x + 1.86$, $R^2 = 0.99$).

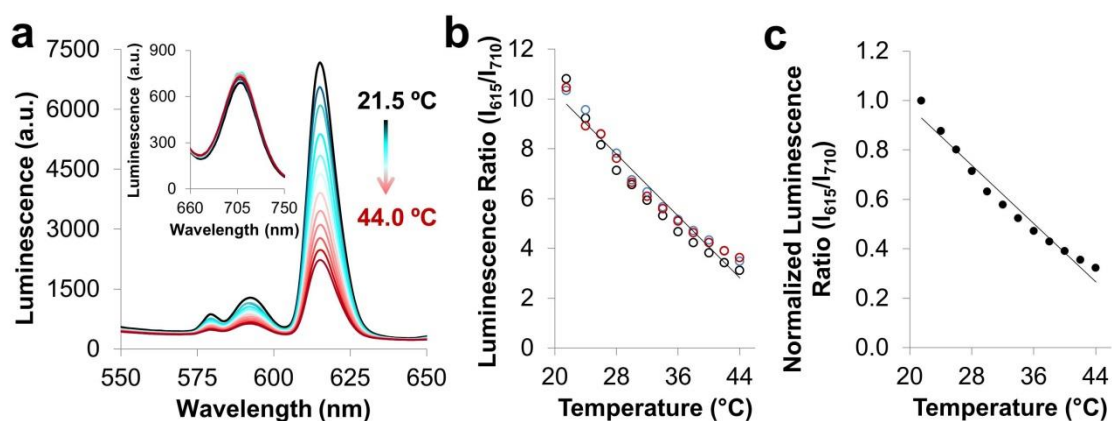


Figure S5. The *in vitro* normalized luminescence ratio (I_{615}/I_{710}) plotted against the varied temperatures (21.5 to 44.0 °C). (a) EuDT emission spectra ($\lambda_{\text{ex}} = 400$ nm) of the RNT at the varied temperatures. Inset: Rhodamine 800 emission spectra ($\lambda_{\text{ex}} = 635$ nm) of the RNT. (b) The ratio of luminescence intensity of EuDT to that of rhodamine 800 (I_{615}/I_{710}) was plotted ($n = 3$ trials, different colours represent independent trials) against the varied temperatures. The temperature sensitivity or the gradient of the averaged data (black line) is $-0.31/^\circ\text{C}$ ($y = -0.31x + 16.45$, $R^2 = 0.97$). (c) The ratio at each temperature was normalized by the ratio at 21.5 °C. The temperature sensitivity of the normalized ratio is $-3.0\%/^\circ\text{C}$ relative to 21.5 °C ($y = -0.030x + 1.56$, $R^2 = 0.97$).

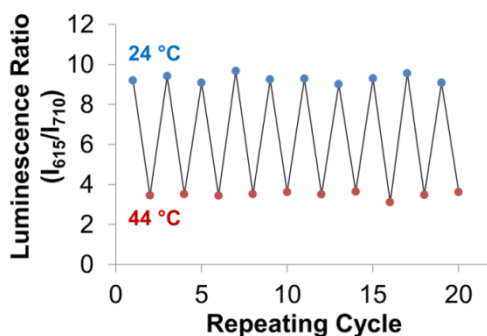


Figure S6. The reversibility of the RNT response against the heating-cooling cycle between 24 °C (blue circles) and 44 °C (red circles). For the EuDT channel, the excitation wavelength was 400 nm and the emission was recorded from 550 to 650 nm, while for the rhodamine 800 channel, the excitation wavelength was 635 nm and the emission was recorded from 660 to 750 nm. The luminescence ratio (I_{615}/I_{710}) was plotted against the number of heating-cooling cycle.

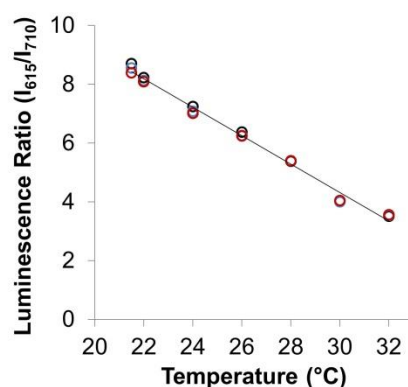


Figure S7. Reversibility of the luminescence ratio (I_{615}/I_{710}) of the RNT under N_2 saturated solution. The ratio of luminescence intensity of EuDT to that of rhodamine 800 (I_{615}/I_{710}) was plotted ($n = 3$ trials, different colours represent independent trials) plotted against the temperature. The temperature sensitivity or the gradient of the averaged data (black line) is $-0.48/^\circ\text{C}$ ($y = -0.48x + 18.83$, $R^2 = 0.99$).

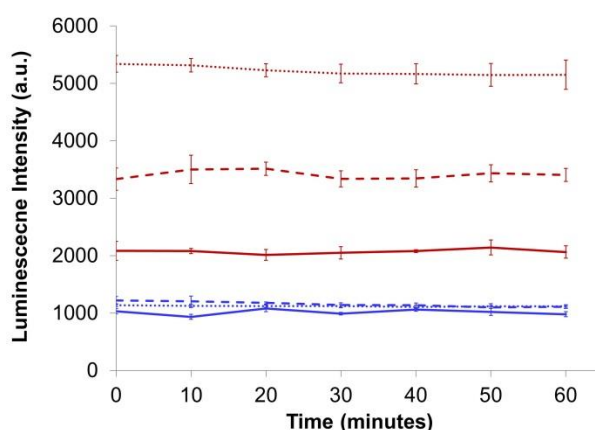


Figure S8. Stability of the RNT at higher temperatures for 60 minutes observation. Luminescence intensity of the RNT in PBS buffer recorded for EuDT (I_{615}) at 50 °C (red solid line), 40 °C (red dashed line), and 30 °C (red dotted line) as well as for rhodamine 800 (I_{710}) at 50 °C (blue solid line), 40 °C (blue dashed line), and 30 °C (blue dotted line), plotted against time. The vertical bar represents the range of the intensities at different measurement trials ($n = 3$ trials). The insignificant variation in the intensities of EuDT and rhodamine 800 in the RNT recorded at high temperature indicates that both dyes were stable and did not leak out from the particles. If EuDT were to leak out, the intensity would drop as EuDT shows attenuated emission in aqueous solution (Fig. S2). If rhodamine 800 were to leak out, the ratio value in Fig. S7 would fluctuate during the heating and cooling cycle and not reversibly respond to the varying temperature; but throughout all the experiments, the ratio value was reversibly responded.

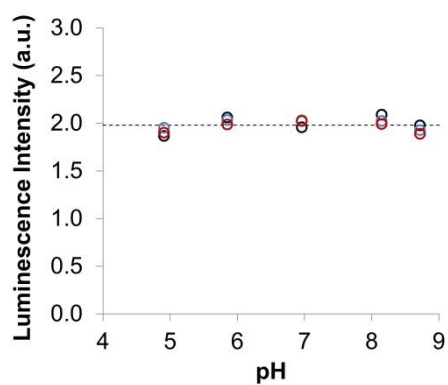


Figure S9. Stability of the RNT in MOPS (3-(*N*-morpholino)propanesulfonic acid) buffer with different pH (5-9). The ratio of luminescence intensity of EuDT to that of rhodamine 800 (I_{615}/I_{710}) was plotted ($n = 3$ trials, different colours represent independent trials) against the varied pH of the buffer solution.

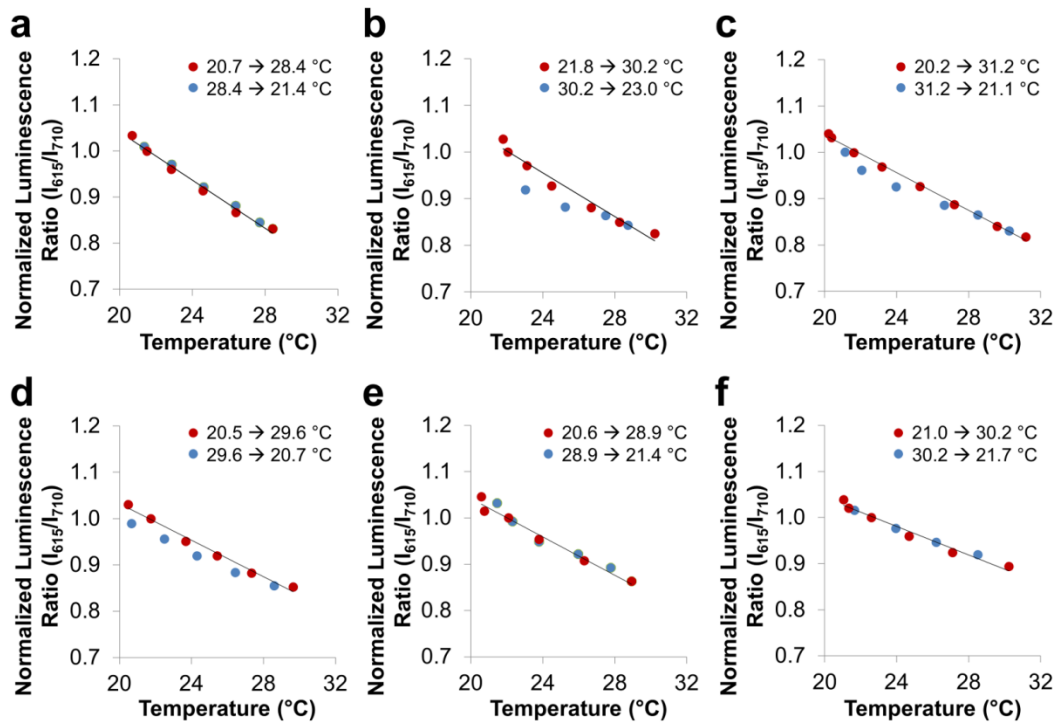


Figure S10. The averaged *in vivo* normalized luminescence ratio (I_{615}/I_{710} , $n = 24$ ROIs) plotted against the varying temperature from flight muscles of different beetles during the heating (red circles) and cooling (blue circles). The relative temperature sensitivities, or the gradient of the normalized ratio value curves during heating, and the temperature by which the normalization was carried out were as follows: (a) $-2.6\%/^{\circ}\text{C}$ relative to 21.5°C ($y = -0.026x + 1.6$, $R^2 = 0.99$); (b) $-2.3\%/^{\circ}\text{C}$ relative to 22.1°C ($y = -0.023x + 1.5$, $R^2 = 0.97$); (c) $-2.0\%/^{\circ}\text{C}$ relative to 21.6°C ($y = -0.020x + 1.4$, $R^2 = 0.99$); (d) $-2.0\%/^{\circ}\text{C}$ relative to 21.7°C ($y = -0.020x + 1.4$, $R^2 = 0.99$); (e) $-2.1\%/^{\circ}\text{C}$ relative to 22.1°C ($y = -0.021x + 1.4$, $R^2 = 0.98$); (f) $-1.6\%/^{\circ}\text{C}$ relative to 22.6°C ($y = -0.016x + 1.4$, $R^2 = 0.97$). The *in vivo* calibrations were carried out after the temperature measurements of the natural preflight preparation process.

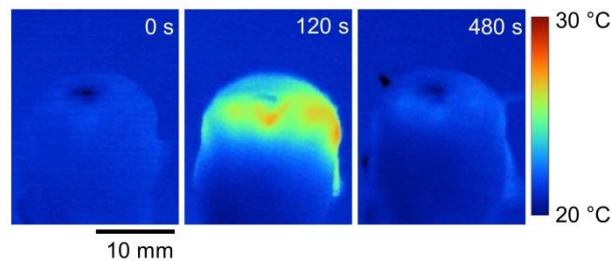


Figure S11. Infrared thermogram of beetle flight muscle during the preflight preparation, 2 days after RNT loading. The preflight preparation is still observed, even 2 days after application of the RNT onto the flight muscles, indicating that the RNT displays non-detectable lethality on the beetle.

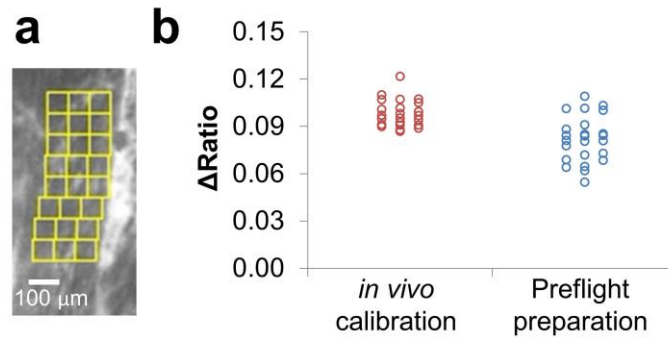


Figure S12. The spreading of the normalized ΔR values, or the difference of maximum and minimum values of the normalized intensity ratio, measured at 24 different ROIs under similar temperature change (ΔT). The ratio at each temperature in both the *in vivo* calibration and the preflight preparation was normalized by the ratio at 22.9 °C. (a) Locations of the 24 ROIs for analysis. (b) Distribution of the normalized ΔR values during the heating process of the *in vivo* calibration (red open circles) and the preflight preparation (blue open circles) under a same temperature range (22.9 to 26.4 °C). The *F*-test showed that the *in vivo* calibration (mean $\Delta R = 0.098 \pm 0.0085$) and the preflight preparation (mean $\Delta R = 0.082 \pm 0.0014$) to have unequal variance ($F = 2.7534 > F_{0.025, 24, 24} = 2.0144$ at a 0.05 significance level) which suggests that the heat production and/or heat transfer significantly differ site-by-site in the preflight preparation as compared to the uniform heating in the *in vivo* calibration.